Int. J. Metrol. Qual. Eng. **14**, 12 (2023)

https://doi.org/10.1051/ijmqe/2023010

International Journal of Metrology and Quality Engineering

Available online at:
www.metrology-journal.org

RESEARCH ARTICLE OPEN ACCESS

Perpendicularity assessment and uncertainty estimation using coordinate measuring machine

Nabil Habibi*, Abdelilah Jalid, Abdelouahab Salih, and Mohamed Zeriab Es-sadek

Mohammed V University of Rabat, ENSAM Rabat, PCMT Laboratory, Avenue de l'Armée Royale, 10100 Rabat Maroc, Morocco

Received: 7 April 2023 / Accepted: 10 July 2023

Abstract. The validation of the conformity of parts according to the ISO 98-4 standard, cannot be achieved without an accurate estimation of the measurement uncertainty, which can become difficult when it comes to a complex measurement strategy to control a geometrical specification of a mechanical part using a Coordinate Measuring Machine (CMM). The purpose of the study in this paper is to analyze the measurement strategy following the Geometric Product Specification (GPS) Standard, to estimate the associated uncertainty of the different parameters of each step, to be able to achieve the uncertainty of the measurement of a given specification (perpendicularity error in our study) using the Guide to the expression of uncertainty in measurement (GUM). This uncertainty will be thereafter validated by a Monte Carlo simulation, and an interlaboratory comparison will be conducted to compare the obtained results according to the ISO 13528 standard. Our contribution is based on a more accurate estimation of the measurement strategy's parameters uncertainties. This approach can also be used by accredited calibration laboratories (ISO 17025) or in the general case in the control of perpendicularity specification of mechanical parts using a coordinate measuring machine. A case study has been conducted, controlling a perpendicularity specification with a tolerance limit of 15 μm, after the calibration of the CMM to obtain the variance-covariance matrices. The mechanical part perpendicularity error (12.55 μm) was below the limit, however, was judged "not conform" when considering the estimated uncertainty (4.06 μm) and the interlaboratory comparison was satisfactory despite the difference of the acceptance criterion.

Keywords: Measurement strategy / coordinate measuring machine (CMM) / ISO/IEC Guide 98-4 / perpendicularity error uncertainty / Geometric Product Specification (GPS / ISO 1101) guide to the expression of uncertainty in measurement (GUM) / Interlaboratory Comparison (ISO 13528) / Monte Carlo simulation (MCS) / ISO 17025

1 Introduction

Coordinate measuring machines are very popular in the industrial field; it allows controlling dimensional and geometrical specifications of complex mechanical parts with great accuracy and precision of less than 1μm. Both hardware and software work simultaneously to collect and process data to generate measurement reports, hence the importance of estimating the uncertainty associated with the measurement. Equipped with a probing system, and following a specific measurement strategy, it collects the coordinates of the tolerance features, then proceeds to the surface fitting according to a given criterion, least-squares method in our case, then proceeds to the verification of a dimensional or geometrical specification. This succession of steps is subject to a propagation of uncertainties, and if not estimated correctly, can lead to aberrant decisions. Evaluating the CMM's measurement-associated uncertainty is a challenging task, especially when examining geometrical error specifications, mainly due to the large number of factors that influence the measurement (Fig. 1).

Several studies have been made to estimate the influence of these parameters on the coordinate measuring machine's measurement uncertainty, such as geometric errors that goes up to 5.63 arcsec following the Y axis for Zeiss Opton CMM with a maximum permissible error of $1.3\,\mu m + \frac{L}{350}$ [1], measuring probe errors estimated around almost $\pm 0.9\,\mu m$ for TP2 Renishaw probe head [2,3], thermal influence errors [4,5] that should be reduced by regulating the temperature homogeneously to $20 \pm 1\,°C$, with a variation less than 0.5 °C per hour and less than 0.5 °C/m height, measurement strategy and fitting criterion [6] that are proven to show minimal influence by probing every 1/10 of the dimension of the surface feature, position, size and shape for point cloud data [7,8]. Rosenda et al. [9] proposed a simplified model, considering these parameters, to estimate the circularity and cylindricity measurement

* Corresponding author: nabil_habibi@um5.ac.ma

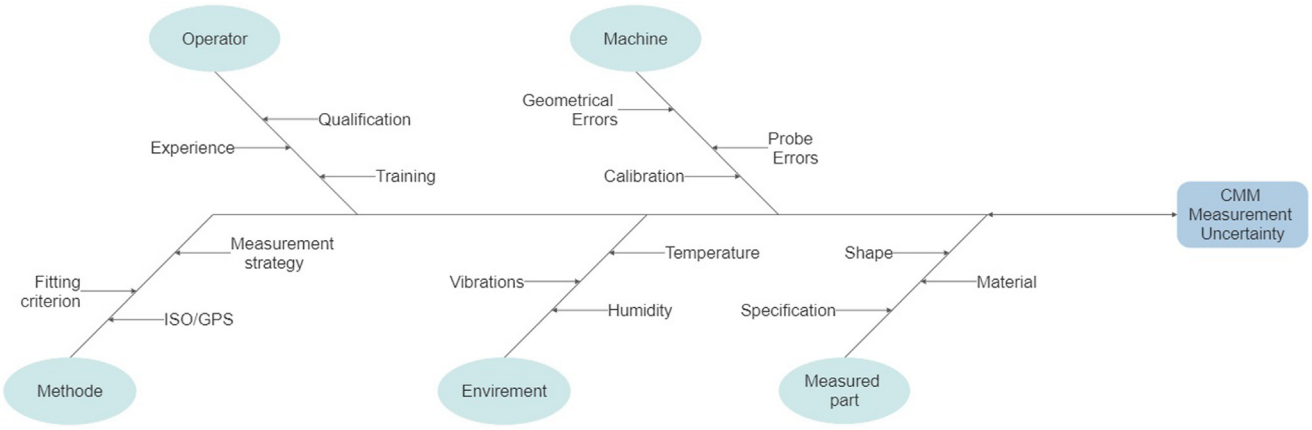

Fig. 1. CMM uncertainty sources.

uncertainty using a coordinate measuring machine. Other studies have been oriented toward estimating the uncertainty of geometrical specifications. Wojciech et al. [10,11] developed different models for size, distance, angle, and geometrical deviation measurement uncertainty, including perpendicularity, fully consistent with the GPS [12] norm. Our contribution is positioned in this context, we seek to estimate the uncertainty of the orientation error following a measurement strategy that respects the normative guidelines.

The GUM and the Monte Carlo method are generally used to estimate the measurement uncertainty. Balasubramanian et al. [13] estimated uncertainty in angle measurement using the GUM considering the geometrical errors, temperature, vibrations, and measuring strategy. Moona et al. [14] developed a model using the Monte Carlo method to estimate the uncertainty for length measurement errors using an articulated arm coordinate measuring machine. Using a comparison between the GUM [15] approach and a Monte Carlo simulation [16] as a validation method has proven to give consistent results, it's within this framework that Jalid [17,18] proposed a comparison of these two methods estimating flatness uncertainty which showed satisfactory results with a gap less than 10^{-4}mm, then studied the influence that sample size has on it.

In this paper, we aim to review the process of validating the conformity of the mechanical parts inspected using CMM, by introducing and considering the measurement uncertainty as stated in the ISO/IEC Guide 98-4 [19]. Our model combines the experimental and the analytical methods to estimate the measurement associated uncertainty. The advantage of this approach is that the perpendicularity uncertainty can be estimated directly from the set of measured points and the calibration of the CMM. It is important to mention too that the uncertainty varies according to the number and position of the measured points and the chosen fitting criterion. To estimate the measurement-associated uncertainty, a deconstruction of the process has been realized, by identifying the different steps of the measurement strategy following the ISO 1101 [12] standard (GPS), and by estimating the variance-covariance matrices at the level of each step by considering the parameters which influence the results, to be able to estimate the final uncertainty of the measurement. This uncertainty will be thereafter validated by a Monte Carlo simulation, before finally proceeding to an inter-laboratory comparison to compare the obtained results. Our contribution is based on a more accurate estimation of the measurement strategy's parameters uncertainties. This approach can be used by ISO 17025 [20] laboratories in the control of perpendicularity specification of mechanical parts using a CMM.

2 Materials and methods

To validate the conformity of a mechanical part using a coordinate measuring machine according to the ISO 98-4 standard, an estimation of the measurement-associated uncertainty is necessary, which can be particularly problematic considering the measurement strategy, mainly due to the number of unknown parameters that can influence the measurement. To do so, we studied a perpendicularity case following this approach:

- Setting a perpendicularity error equation according to the ISO 1101 standard (GPS).
- Estimation of the perpendicularity error associated uncertainty.
- Validation of the proposed method.
- Declaration of conformity according to the ISO 98-4 standard.

A verification of our results through an inter-laboratory comparison according to the ISO 13528 standard will be accomplished in the results and discussion section.

2.1 Perpendicularity error modeling

Based on the Geometric Product Specification (ISO 1101 standard) [12], perpendicularity is an orientation tolerance; and can be defined as the minimum distance between two theoretical parallel elements, both perpendicular to the datum, within which all measured points lie inside, whether it is a plane or axis (Fig. 2).

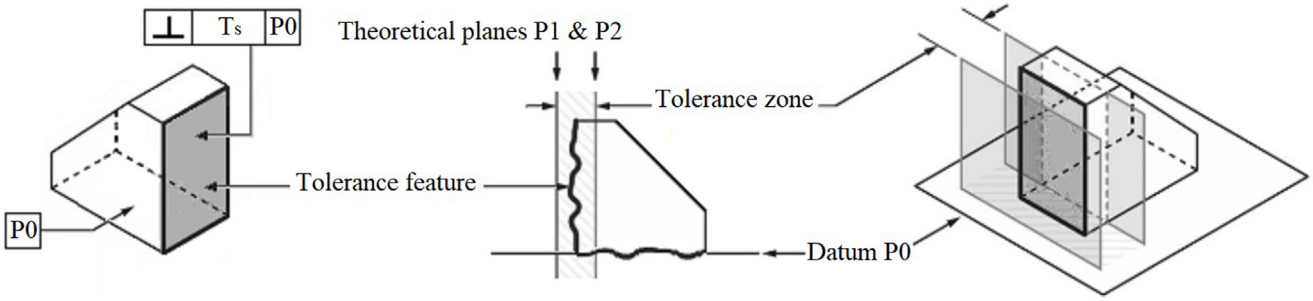

Fig. 2. Perpendicularity error.

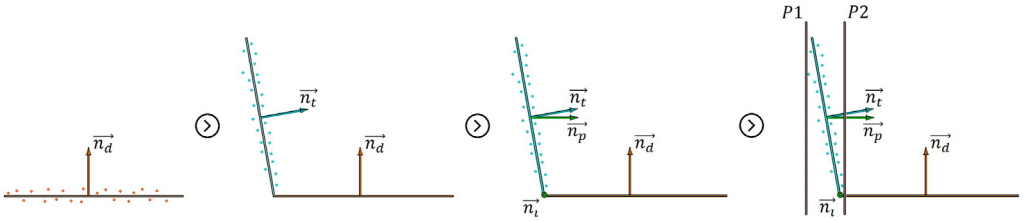

Fig. 3. Measurement strategy steps.

We have studied a plane-to-plane perpendicularity case, the geometrical specification was summarized as follows:

- *Tolerance feature:* probed points that belong to the tolerance surface.
- *Datum:* theorical fitted plane P0.
- *Tolerance zone:* Volume between two theorical parallel planes P1 and P2, both perpendicular to the datum.
- *Condition:* all probed points must lie inside the tolerance zone.

2.1.1 Measurement strategy

The measurement strategy using CMM should be carefully planned and executed to achieve the desired level of accuracy and comply with the GPS norm. In order to measure the perpendicularity error, we applied the following strategy (Fig. 3).

Probing the datum surface then fitting a theorical plane using the least-squares method, the choice of the number of measured points and fitting criterion has been chosen to represent the best the surface [6], then extracting the datum's associated plane normal vector $\overrightarrow{n_d}$. Probing the tolerance element using the same method and extracting the measured points coordinates as well as the tolerance surface associated plane normal vector $\overrightarrow{n_t}$. It is important to mention that $\overrightarrow{n_d}$ and $\overrightarrow{n_t}$ are not necessarily perfectly perpendicular, hence the need to calculate the vector $\overrightarrow{n_p}$. Calculating the datum and tolerance planes intersection vector $\overrightarrow{n_i} = \frac{\overrightarrow{n_d} \wedge \overrightarrow{n_t}}{\overrightarrow{n_d} \wedge \overrightarrow{n_t}}$ to be able to calculate the vector $\overrightarrow{n_p} = \overrightarrow{n_d} \wedge \overrightarrow{n_i}$. Calculating the two most distant measured points p_{max} and p_{min} along the vector $\overrightarrow{n_p}$, allowing us to set the planes P1 (p_{max}, $\overrightarrow{n_p}$) and P2(p_{min}, $\overrightarrow{n_p}$), and deducting the perpendicularity error (Fig. 4).

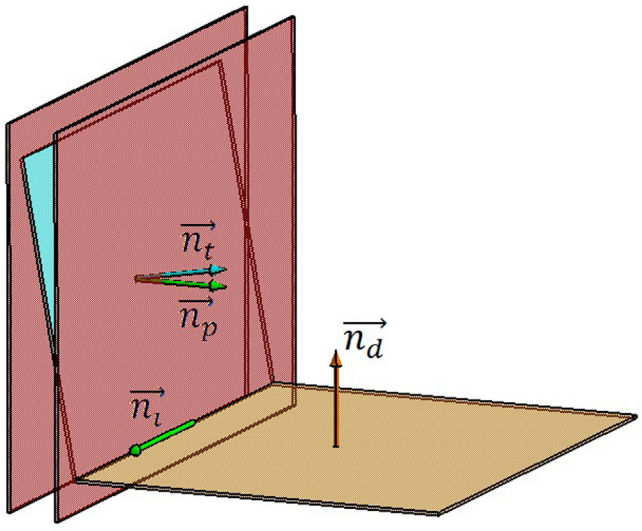

Fig. 4. Construction of the tolerance zone.

This succession of steps is subject to a propagation of uncertainties, and if not estimated correctly, can lead to a false conformity declaration. According to equation (1), and following this measurement strategy, the main sources of the perpendicularity measurement uncertainty are the probed points, the associated datum normal vector and the intersection vector. In the following Section, we will quantify the uncertainties associated with these parameters for each step of the measurement strategy. Forbes [21,22] conducted other studies on the estimation of the variance-covariance matrix of the features with a finite set of points dispersed evenly over the surface being sampled, allowing to estimate uncertainties using the GUM method without knowing the measurement strategy, and reducing the effect of form effort, considering only the number of data points and geometry of the area being sampled.

2.1.2 Perpendicularity error

Let p_i be the coordinates of the i^{th} probed point, such as $p_{max}(x_{max}, y_{max}, z_{max}) \in P1$ and $p_{min}(x_{min}, y_{min}, z_{min}) \in P2$ the two most distant measured points, the perpendicularity error can be expressed as follows:

$$dp = |p_{max}\vec{p}_{min}.(\vec{n_d} \wedge \vec{n_e})|. \quad (1)$$

where $\overrightarrow{n_p} = \overrightarrow{n_d} \wedge \overrightarrow{n_e}$ represents the theorical parallel plane's P1 and P2 normal vector, $\overrightarrow{n_d}(n_{dx}, \mathrm{n_{dy}}, \mathrm{n_{dz}})$ the datum plane's normal vector, and $\overrightarrow{n_e}(n_{ex}, \mathrm{n_{ey}}, \mathrm{n_{ez}})$ the vector of the intersection between the datum and tolerance surface (unit vectors). Hence the final expression of the parallelism error:

$$\begin{aligned} dp &= \left| \begin{pmatrix} x_{p_{min}} - x_{p_{max}} \\ y_{p_{min}} - y_{p_{max}} \\ z_{p_{min}} - z_{p_{max}} \end{pmatrix} \begin{pmatrix} n_{dy}n_{ez} - n_{dz}n_{ey} \\ n_{dz}n_{ex} - n_{dx}n_{ez} \\ n_{dx}n_{ey} - n_{dy}n_{ex} \end{pmatrix} \right| \\ &= \left| \begin{array}{c} \left(x_{p_{min}} - x_{p_{max}}\right)\left(n_{dy}n_{ez} - n_{dz}n_{ey}\right) \\ +\left(y_{p_{min}} - y_{p_{max}}\right)\left(n_{dz}n_{ex} - n_{dx}n_{ez}\right) \\ +\left(z_{p_{min}} - z_{p_{max}}\right)\left(n_{dx}n_{ey} - n_{dy}n_{ex}\right) \end{array} \right|. \end{aligned} \quad (2)$$

2.2 Estimation of the perpendicularity error associated uncertainty

In order to estimate the perpendicularity error associated uncertainty using the GUM uncertainty propagation model, we applied the following procedure:

- Applying the GUM method to the perpendicularity equation (1).
- Estimating the parameters and their associated variance-covariance matrix.
- Validation of the GUM results through a Monte Carlo simulation.

2.2.1 GUM uncertainty propagation model

The GUM (Guide to the Expression of Uncertainty in Measurement [15]) variance propagation method is widely used in different fields, especially in metrology, it provides an analytic approach for quantifying and expressing the uncertainty of measurement based on a first-order Taylor expansion of a function through a linear approximation. To estimate the perpendicularity error default uncertainty, the GUM method is applied to the perpendicularity model $dp = f(n_{dx}, n_{dy}, n_{dz}, n_{ex}, n_{ey}, n_{ez}, x_{p_{min}}, y_{p_{min}}, z_{p_{min}}, x_{p_{max}}, y_{p_{max}}, z_{p_{max}})$ in equation (1):

$$\begin{aligned} u_c^2(dp) &= \sum_{i=1}^{N} \left[\left(\frac{\partial dp}{\partial X_i}\right)\right]^2 var(X_i) \\ &+ 2\sum_{i=1}^{N-1}\sum_{j=i+1}^{N} \left(\frac{\partial dp}{\partial X_i}\right)\left(\frac{\partial dp}{\partial X_j}\right) cov(X_i, X_j) \\ &= \sum_{i=1}^{N}\sum_{j=1}^{N} \left(\frac{\partial dp}{\partial X_i}\right)\left(\frac{\partial dp}{\partial X_j}\right) cov(X_i, X_j) = JMJ^T. \end{aligned} \quad (3)$$

The modeling in matrix form will allow us thereafter to implement the calculations on Matlab, where J represents the Jacobian matrix:

$$J = \left[\begin{array}{c} \frac{\partial dp}{\partial n_{dx}} \frac{\partial dp}{\partial n_{dy}} \frac{\partial dp}{\partial n_{dz}} \frac{\partial dp}{\partial n_{ex}} \frac{\partial dp}{\partial n_{ey}} \frac{\partial dp}{\partial x_{ez}} \frac{\partial dp}{\partial x_{pmin}} \frac{\partial dp}{\partial y_{pmin}} \\ \frac{\partial dp}{\partial z_{pmin}} \frac{\partial dp}{\partial x_{\mathrm{pmax}}} \frac{\partial dp}{\partial y_{\mathrm{pmax}}} \frac{\partial dp}{\partial z_{\mathrm{pmax}}} \end{array} \right] \quad (4)$$

And M represents the uncertainty variance-covariance associated matrix:

$$M = \begin{pmatrix} \left[\overrightarrow{n_d}\right] & \cdots & \cdots & [0] \\ \vdots & \left[\overrightarrow{n_e}\right] & \ddots & \vdots \\ \vdots & \ddots & [p_{min}] & \vdots \\ [0] & \cdots & \cdots & [p_{max}] \end{pmatrix} \quad (5)$$

where the terms $\left[\overrightarrow{n_d}\right], \left[\overrightarrow{n_e}\right], [p_{min}], [p_{max}]$ are respectively the associated variance-covariance matrix of the variables $\overrightarrow{n_d}, \overrightarrow{n_e}, p_{min}, p_{max}$.

2.2.2 Estimation of the parameters associated variance-covariance matrix

Coordinate measuring machines are precise and accurate. However, various factors influence the measurement uncertainty (Fig. 1), and it is very difficult to quantify the influence of each of these parameters independently of the others. Several approaches have been made, Bahassou et al. [23,24] proposed an estimation of the variances according to the ISO 10360 standard [25]. We will assume that the errors along the axes are independent and linear:

$$[p_{min}] = [p_{max}] = \begin{pmatrix} u_x & 0 & 0 \\ 0 & u_y & 0 \\ 0 & 0 & u_z \end{pmatrix}. \quad (6)$$

Thereby measuring 5 gauge blocks, each block for 3 repetitions, along 3 of the 7 directions (Fig. 5), then calculating the error equations along each direction $E_x = A_x x + B_x$ (error following the direction X for example), Then applying the law of propagation of uncertainties to estimate the associated uncertainty u_x.

Surface fitting is a critical step. To estimate the variance-covariance matrix associated to the datum normal vector, we must first select a mathematical model to associate the set of probed points to an ideal plane, representing the measured surface without overfitting or underfitting. It may be done using a variety of techniques, such as polynomial fitting, radial basis functions, and splines, each method has advantages and disadvantages. Several criteria [6] of surface fitting are commonly used and comply with the norms, of which we can mention: The least-squares method, it consists of minimizing the sum of squared residuals: $min\sum_{i=1}^{N} e_i^2$ where $e_i = \vec{Ap_i}.\vec{n}$ such as

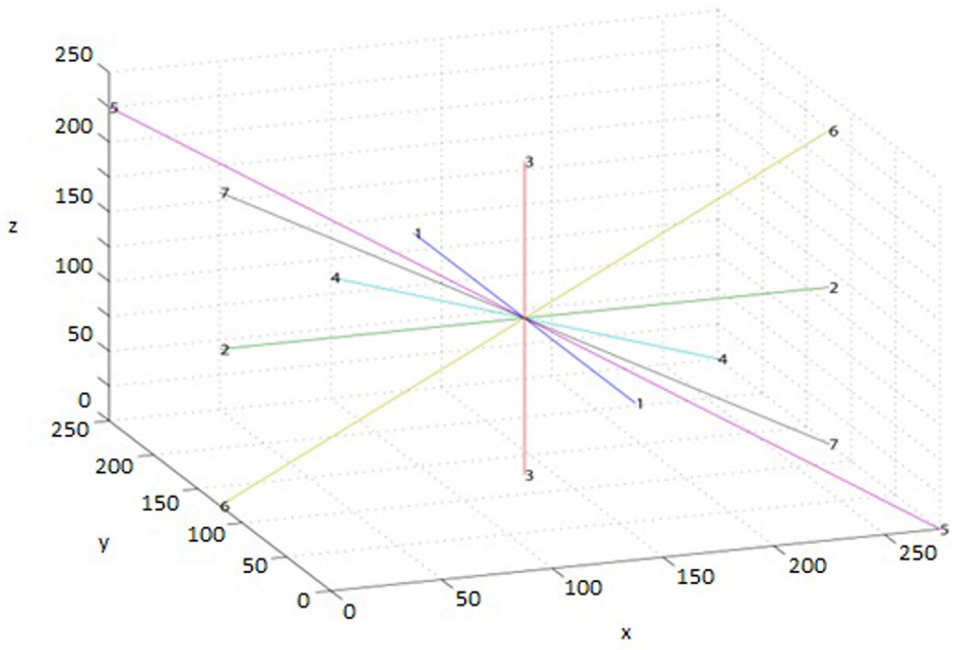

Fig. 5. The ISO 10360 directions.

$(\mathrm{A}, \vec{n})$ are the substitute plane parameters and P_i are the measured points.. And the Chebyshev criterion, minimizing the maximum absolute difference from the data points to the fitted surface: $\underset{p_i}{min}\left(\underset{1\leq i\leq N}{\max} e_i\right)$ (Fig. 6).

The least-squares method tends to be more sensitive to outliers in the data because it squares the errors. Large errors have a more significant impact which provides a good overall fit to the data but may not guarantee the smallest maximum error across the entire data range. While the Chebyshev approximation method is less sensitive to outliers because it focuses on the maximum absolute error providing a more accurate fit in terms of the worst-case scenario but potentially sacrificing the overall fit. The choice between these methods depends on the specific requirements of the problem, the characteristics of the data, and the desired trade-off between overall fit and worst-case accuracy. For the rest of this study, we will refer to the least-squares consisting of minimizing equation (7):

$$\begin{aligned} e_i^2 &= \left[\begin{pmatrix} x_{p_i}-x_A \\ y_{p_i}-y_A \\ z_{p_i}-z_A \end{pmatrix}\begin{pmatrix} n_x \\ n_y \\ n_z \end{pmatrix}\right]^2 \\ &= \left[(x_{p_i}-x_A)n_x + \left(y_{p_i}-y_A\right)n_y + \left(z_{p_i}-z_A\right)n_z\right]^2. \quad (7) \end{aligned}$$

To solve this equation, we used the "nlinfit" function in Matlab, which requires starting parameters $(A_0, \overrightarrow{n_0})$. To achieve a stable result and avoid local solutions, we have chosen the center of mass of the measured points $A_0\left(\frac{\sum x_{p_i}}{n}, \frac{\sum y_{p_i}}{n}, \frac{\sum z_{p_i}}{n}\right)$ and an initial normal vector $\overrightarrow{n_0} = \frac{\overrightarrow{ab}\,\overrightarrow{ac}}{|\overrightarrow{ab}\overrightarrow{ac}|}$ based on the most distant probed point apart a, b and c.

Once the associated plane $(A,\ \vec{n})$ is estimated, we proceed to the estimation of the variance-covariance matrix associated with a $\vec{n}\,(x_o, y_o, z_o)$. The objective of the introduction of this matrix, is to highlight the influence of the measurement strategy parameters: the chosen fitting criterion (LSM) as well as the number and distribution of the probed points, based on the principle that the greater the number and of points probed and the larger their coverage, the more we converge to the normal that better represents the real surface, assuming that it follows a normal distribution of the form:

$$F(\overrightarrow{n_i}) = \frac{1}{\sigma\sqrt{2\pi}} e^{\left(\frac{n_i - n_o}{\sigma}\right)^2}. \quad (8)$$

We will not consider the influence of the uncertainty associated with the probed points, being already taken into account in the matrix $[P_i]$ above (Eq. (6)). The feature is measured for N repetitions, and we then estimate the normal vector for each sample using the least-squares algorithm coded above, before calculating their variance-covariance referring to the following equations:

$$\begin{cases} cov(y,z) = \frac{1}{N-1}\sum_{i=1}^{n}(y_i - y_o)(z_i - z_o) \\ \mathrm{var(x)} = \frac{1}{N-1}\sum_{i=1}^{n}(x_i - x_o)^2 \end{cases}$$

Following this procedure above, we developed an algorithm on Matlab, starting from a set of data points, proceeding to the fitting process using the least-squares method then giving us the fitted datum plane parameters $(A,\ \overrightarrow{n_d})$ and its variance-covariance matrix associated

Fig. 6. Surface fitting.

with the associated measurement strategy:

$$\left[\overrightarrow{n_d}\right] = \begin{pmatrix} var(n_{dx}) & cov(n_{dx}, n_{dy}) & cov(n_{dx}, n_{dz}) \\ cov(n_{dy}, n_{dx}) & var(n_{dy}) & cov(n_{dy}, n_{dz}) \\ cov(n_{dz}, n_{dx}) & cov(n_{dz}, n_{dy}) & var(n_{dz}) \end{pmatrix}. \tag{9}$$

Regarding the intersection vector $\overrightarrow{n_i}$, representing the direction of the intersection between the datum and tolerance planes, expressed as follows:

$$\left[\overrightarrow{n_e}\right] = \frac{1}{||\overrightarrow{n_d} \wedge \overrightarrow{n_t}||} \begin{pmatrix} n_{dy}n_{tz} - n_{dz}n_{ty} \\ n_{dz}n_{tx} - n_{dx}n_{tz} \\ n_{dx}n_{ty} - n_{dy}n_{tx} \end{pmatrix}. \tag{10}$$

We will assume that $\sin\left(\overrightarrow{n_d}, \overrightarrow{n_t}\right) \simeq 1$, and we apply the law of propagation of uncertainties on each term of the vector:

$$\begin{aligned} u_c^2(n_{e,x}) = {} & {n_{dy}}^2 var(n_{tz}) + {n_{tz}}^2 var(n_{dy}) \\ & + {n_{dz}}^2 var(n_{ty}) + {n_{ty}}^2 var(n_{dz}) \\ & + 2n_{dy}n_{dz}cov(n_{ty}, n_{tz}) \\ & + 2n_{ty}n_{tz}cov(n_{dy}n_{dz}). \end{aligned} \tag{11}$$

Similarly, for $u_c^2(n_{e,y})$ and $u_c^2(n_{e,z})$, to reach the final form of the variance-covariance matrix:

$$\left[\overrightarrow{n_i}\right] = \begin{pmatrix} v_{x,n_e} & 0 & 0 \\ 0 & v_{y,n_e} & 0 \\ 0 & 0 & v_{z,n_e} \end{pmatrix}. \tag{12}$$

Once the estimation of the variance-covariance matrix of each parameter is done, respectively $[p_{min}], [p_{max}], \left[\overrightarrow{n_d}\right], \left[\overrightarrow{n_e}\right]$, we will obtain the final form of the matrix [M] (Eq. (5)).

2.2.3 Monte Carlo simulation

The estimation of measurement uncertainty using a Monte Carlo simulation [16] is a great alternative especially when other methods present some difficulties such as an inadequate linearization of the model resulting in unrealistic confidence intervals. It's a statistical propagation of distributions that uses random sampling through a mathematical model to determine the range of possible outcomes allowing us therefore to estimate the model's uncertainty. A Monte Carlo simulation could also be used to compare and validate the results using the GUM method following this procedure.

Calculating the limits of the confidence interval $dp_{low_{GUM}}$ and $dp_{high_{GUM}}$ resulting from the application of the GUM method, where "dp" represents the nominal value of the perpendicularity error and $U(dp)$ it's associated uncertainty:

$$\begin{cases} dp_{low_{GUM}} = dp - U(dp) \\ dp_{high_{GUM}} = dp + U(dp) \end{cases}$$

Running a Monte Carlo Simulation and extracting from the generated distribution both perpendicularity error mean value and its deviation, to be able to calculate $dp_{low_{MCS}}$ and $dp_{high_{MCS}}$ as they represent the limits for a 95.45% confidence interval $(dp \pm 2\sigma)$, then comparing the GUM and Monte Carlo confidence interval limits:

$$\begin{cases} d_{low} = |dp_{low_{GUM}} - dp_{low_{MCS}}| \\ d_{high} = |dp_{high_{GUM}} - dp_{high_{MCS}}| \end{cases}$$

Setting the numerical tolerance $\zeta = 0.5x10^{r}$where "r" is expressing the necessary number of accurate decimal digits. Then if the condition $\zeta \geq max\,(d_{low}, d_{high})$ is verified, the comparison is favorable, meaning that GUM framework has been validated in this instance.

2.3 Declaration of the conformity

The conformity assessment is a critical step, it can decide whether the mechanical part conforms to the given specification. If the measurement uncertainty is not considered, it can lead to aberrant decisions, especially if the measurement result is close to the specification limit. CMMs can automatically generate a conformity report based on the specification tolerance interval. If we take the perpendicularity as an example, the CMM validity assessment follows this procedure: $\begin{cases} if dp \leq T_L \; validation \\ if dp > T_L \; rejection \end{cases}$ where T_L represents the specification/tolerance limit (Fig. 7).

If we consider the uncertainty, two forms of incorrect decisions would appear inside the uncertainty zone. False acceptance, which is validating the non-conform specification part, known as consumer's risk. And false rejection, which is rejecting a conform specification part, also known as producer's risk (respectively Type I (α) and Type II (β) errors). The decision-making process was significantly impacted by the development of a probabilistic approach, introducing measurement uncertainty as a conformity parameter (Fig. 8).

To establish a conformity validation procedure associated with the measured dimensional or geometrical specifications, it will be necessary to calculate the risk zone, assuming that the uncertainty follows a normal distribution:

$$\emptyset(x) = \int_{x}^{+\infty} F(Z)dZ. \tag{13}$$

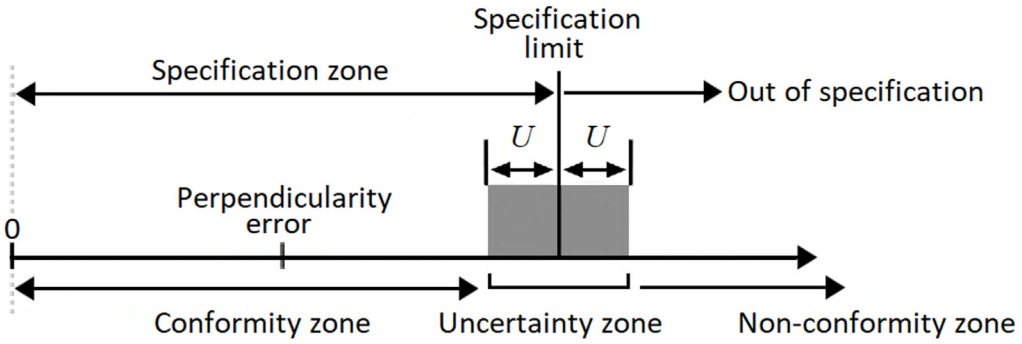

Fig. 7. Conformity assessment.

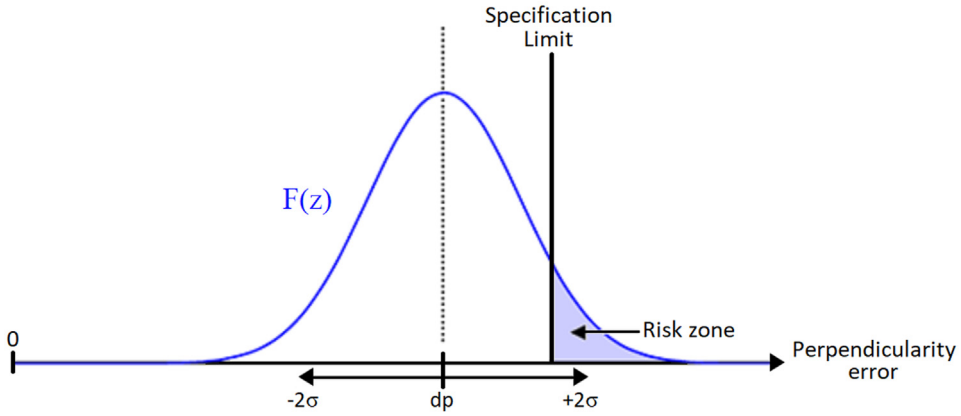

Fig. 8. Perpendicularity error uncertainty distribution.

According to the ISO/IEC Guide 98-4 [17], if the tolerated risk limit is not specified by the customer, the risk $p_\alpha = \{dp > z_i\} = 1 - \emptyset\,(z_i)$ should not exceed 2.3%. Where z_i is the Gaussian coefficient using the standard normal distribution expressed as follows: $z_i = \frac{Ts-dp}{U/2}$.

3 Results and discussion

This experimental study aims to bring the previously developed theoretical model into practice. The tests were carried out in the PCMT metrology laboratory where the temperature is regulated at around $20 \pm 2\,°C$, the coordinate measuring machine used is a Mitutoyo Euro-C 544 coupled to a TP2 type probing head on which is mounted a Tungsten Carbide stylus of effective working length EWL = 14 mm and D=2 mm ruby ball diameter, altogether driven by Geopak software. The maximum permissible error is $E_{L,MPE} = \pm\,(4\mu m + L/200)$ with L in mm. The geometrical specification being studied is a perpendicularity error with a tolerance limit of 15 µm:

We started by estimating the variance-covariance matrix associated to this CMM's measured points by applying the GUM method to the error equations following the ISO 10360 directions [23,24]:

$$[p_i] = 10^{-6}\begin{pmatrix} 6.6125 & 0 & 0 \\ 0 & 7.812 & 0 \\ 0 & 0 & 4.052 \end{pmatrix} \text{mm}.$$

Most of researchers use uncertainties based on the MPE. The main purpose of the variance matrix proposed, is to make good use of the ISO 10360 calibration results of the CMM, generating a correction matrix and a plausible variance matrix consistent with the MPE statement (Fig. 9).

To control the mechanical part, we referred to the steps described in Section 2.2, we probed the reference plane, then the specified plane, it is important to note that in order to minimize probing error, the probe must be oriented in the same orientation as the normal vector while measuring all the data points (Tab. 1).

After extracting the cloud of points, we then proceeded to the construction of the required vectors as shown in Table 2:

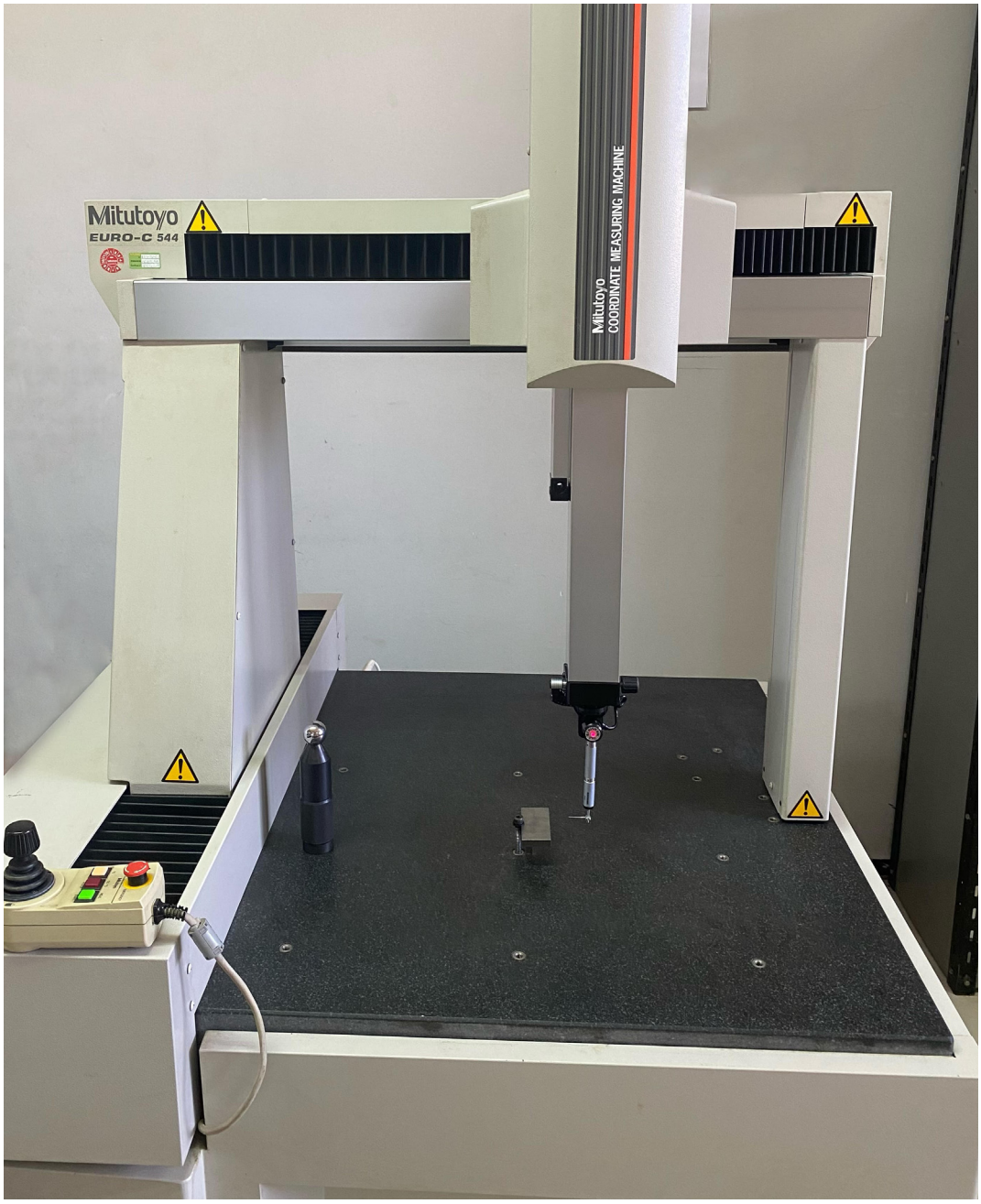

Fig. 9. Used CMM.

Then constructing the tolerance zone between

$$P1 = \left(\begin{pmatrix} 9995 \\ 9998 \\ 50001 \end{pmatrix}, \begin{pmatrix} -0.\vec{99999997} \\ -2.4263\mathrm{E}-05 \\ 1.0181\mathrm{E}-04 \end{pmatrix} \right)$$

$$\text{and } P2 = \left(\begin{pmatrix} 10003 \\ 30001 \\ 10001 \end{pmatrix}, \begin{pmatrix} -0.\vec{99999997} \\ -2.4263\mathrm{E}-05 \\ 1.0181\mathrm{E}-04 \end{pmatrix} \right)$$

to be able to evaluate the perpendicularity error:

$$dp = |p_{max}\vec{p}_{min}.(\vec{n_d} \wedge \vec{n_e})| = 12.55\mu\mathrm{m}.$$

It is important to mention that he problem with the ISO 1101 definition of perpendicularity is that the uncertainty associated with the measurement is directly related to the measurement strategy and form error, which influence on the parallelism error considerably.

Table 1. Tolerance plane measured points (in mm).

x	y	z
9. 993	9. 999	9. 999
9. 996	9. 999	25. 001
9. 995	9. 998	50. 001
9. 997	29. 997	50. 003
10. 003	29. 996	37. 003
10. 004	29. 999	22. 999
10. 003	30. 001	10. 001
9. 997	50. 001	9. 999
10. 001	50. 001	25. 002
9. 998	49. 997	50. 004

Table 2. Construction of the vectors (in mm).

Vector	n_x	n_y	n_z
$\overrightarrow{n_d}$	1.01682E-04	-1.0423E-04	0.99999999
$\overrightarrow{n_t}$	0.999999994	2.42410E-05	1.06659E-04
$\overrightarrow{n_e}$	-2.4252E-05	0.999999973	1.04232E-04
$\overrightarrow{n_p} = \overrightarrow{n_d} \wedge \overrightarrow{n_t}$	-0.99999997	-2.4263E-05	1.0181E-04

Table 3. Sample of datum plane normal vectors for 10 repetitions (in mm).

n_x	n_y	n_z
0.000101811	0.000106660	0.999999991
-0.000019393	0.000087266	0.999999996
0.000048481	0.000052418	0.999999995
0.000029089	0.000092115	0.999999995
0.000033937	0.000063026	0.999999997
0.000063026	0.000014544	0.999999998
0.000106659	0.000043633	0.999999994
0.000047152	0.000024241	0.999999994
0.000028908	0.000087266	0.999999996
0.000105925	0.000067874	0.999999997

3.1 GUM application

The perpendicularity error associated uncertainty is obtained by propagating the parameters uncertainty across the measurement strategy process through a linear approximation. By that means, we started by estimating the variance covariance matrix associated to the datum normal vector, which evaluates the influence of the number of probed points and their distribution as a result of the randomization of the measured points to generate the different possible combinations (Tab. 3).

Therefore, allowing us to set the datum normal vector associated variance-covariance matrix:

$$\left[\overrightarrow{n_d}\right] = \begin{pmatrix} 1.6611\text{E}-09 & -2.1262\text{E}-10 & -2.7379\text{E}-14 \\ -2.1262\text{E}-10 & 9.2049\text{E}-10 & -2.29181\text{E}-14 \\ -2.7379\text{E}-14 & -2.2918\text{E}-14 & 4.0111\text{E}-18 \end{pmatrix} \text{mm}.$$

However, it is important to mention that the probing error influence the matrix being based on a repeatability model. An interesting alternative approach to estimate the normal vector associated variance-covariance matrix would be for each "N" probed points $\{p_1, p_2 \ldots . p_N\}$, we proceed to a Monte Carlo randomization of the measured points to generate the different possible combinations, representing the same feature plane, with varied distributions and number of points N with $3 \leq n < N$. We then estimate the normal vector for each sample using a specific fitting criterion, before calculating their variance covariance.

Similarly, we estimated $[\vec{n_t}]$ associated with the tolerance plane's normal vector, to be able to assess the intermediate vector's variance-covariance matrix, representing the direction of the intersection of the two measured planes:

$$[\vec{n_e}] = \begin{pmatrix} 1.6612\text{E}-09 & 0 & 0 \\ 0 & 2.5028\text{E}-17 & 0 \\ 0 & 0 & 9.2048E-10 \end{pmatrix} \text{mm}.$$

Table 4. Results comparison.

GUM results	**Monte Carlo results**
$dp = 0.01255$ mm	$y_{mean} = 0.012551$ mm
$dp - U_{dp} = 0.0084821$ mm	$y_{low} = 0.0085633$ mm
$dp + U_{dp} = 0.0166178mm$	$y_{high} = 0.0165387$ mm
$\sigma_{dp} = 0.00203392$ mm	$\sigma_{MCM} = 0.00199387$ mm
$U_{dp} = 0.00406785$mm	$U_{MCM} = 2\sigma_{MCM} = 0.00398774$mm

Table 5. Conformity assessment.

Perpendicularity error dp	12.55 µm
Perpendicularity measurement uncertainty U_{dp}	4.06 µm
Perpendicularity tolerance limit T_s	15 µm
Gaussian Coefficient z_i	1.20689655 µm
Risk alpha p_α	0.11373599

$$J^T = \begin{pmatrix} \frac{\partial df}{\partial n_{dx}} = (z_{p_{min}} - z_{p_{max}})n_{iy} - (y_{p_{min}} - y_{p_{max}})n_{iz} \\ \frac{\partial df}{\partial n_{dy}} = (x_{p_{min}} - x_{p_{max}})n_{iz} - (z_{p_{min}} - z_{p_{max}})n_{ix} \\ \frac{\partial df}{\partial n_{dz}} = (y_{p_{min}} - y_{p_{max}})n_{ix} - (x_{p_{min}} - x_{p_{max}})n_{iy} \\ \frac{\partial df}{\partial n_{ex}} = (y_{p_{min}} - y_{p_{max}})n_{dz} - (z_{p_{min}} - z_{p_{max}})n_{dy} \\ \frac{\partial df}{\partial n_{ey}} = (z_{p_{min}} - z_{p_{max}})n_{dx} - (x_{p_{min}} - x_{p_{max}})n_{dz} \\ \frac{\partial df}{\partial n_{ez}} = (x_{p_{min}} - x_{p_{max}})n_{dy} - (y_{p_{min}} - y_{p_{max}})n_{dx} \\ \frac{\partial dp}{\partial x_{p_{min}}} = n_{dy}n_{iz} - n_{dz}n_{iy} \\ \frac{\partial dp}{\partial y_{p_{min}}} = n_{dz}n_{ix} - n_{dx}n_{iz} \\ \frac{\partial dp}{\partial z_{p_{min}}} = n_{dx}n_{iy} - n_{dy}n_{ix} \\ \frac{\partial dp}{\partial x_{p_{max}}} = n_{dz}n_{iy} - n_{dy}n_{iz} \\ \frac{\partial dp}{\partial y_{p_{max}}} = n_{dx}n_{iz} - n_{dz}n_{ix} \\ \frac{\partial dp}{\partial z_{p_{max}}} = n_{dy}n_{ix} - n_{dx}n_{iy} \end{pmatrix} = \begin{pmatrix} -4.000208\text{E}+01 \\ 0.00096925\text{E}-04 \\ -8.4851\text{E}-03 \\ -1.999883\text{E}+01 \\ -1.206722\text{E}-02 \\ 2.034779\text{E}-03 \\ -9.999999E-01 \\ -2.4263\text{E}-05 \\ 1.0161\text{E}-04 \\ 9.999999E-01 \\ 2.4263\text{E}-05 \\ -1.0161\text{E}-04 \end{pmatrix} mm.$$

The Jacobian matrix (Eq. (4)) is calculated with the following simplifications:

Consequently, we can estimate the perpendicularity error associated uncertainty using the GUM method developed in Section 2.2.

$$U_{dp} = ku_c(dp) = 2\sqrt{JMJ^T} = 4.06\mu\text{m}.$$

The uncertainty may seem relatively big compared to the error $\frac{U(dp)}{dp} \simeq 32\%$, but it is mainly due to the low perpendicularity default compared to the capability of CMMs used.

3.2 Monte Carlo simulation

We referred to a comparison between the GUM results and a Monte Carlo simulation to validate the perpendicularity uncertainty estimation. The Monte Carlo method can cope with non-smooth input-output models and can be used to evaluate the uncertainty associated with the perpendicularity error. Supposing that the parameters follow a normal law distribution, the simulation was carried out in two stages, the first being to randomize the cloud of probed points, with known mean values and standard deviations $\sigma = U/k$ extracted from their respective variance matrices with $k=2$ as coverage factor, to determine the maximum and minimum points for each sample, followed by a second randomization of the $[\vec{n_d}]$and$[\vec{n_e}]$ vectors, in order to obtain the perpendicularity error output estimated referring to the $(n_{px}, n_{py}, n_{pz}, n_{ex}, n_{ey}, n_{ez}, x_{p_{min}}, y_{p_{min}}, z_{p_{min}}, x_{p_{max}}, y_{p_{max}}, z_{p_{max}})$ parameters.

Figure 10 shows the distribution function obtained when generating a 10^5 sample and 10^3 classes of 0.02 µm:

We extract the following results (Tab. 4).

The numerical tolerance is $\zeta = 0$, 5.10^{-3}mm, and (d_{low}, d_{high}) represent the difference of the limits for a 95.45% confidence interval ($y_{mean} \pm 2\sigma_{MCM}$) of the generated distribution and the GUM method results calculated as follows:

$$\begin{cases} d_{low} = |dp - U_{dp} - y_{low_{MCS}}| \\ 0.791.10^{-4}mm \leq \zeta \\ d_{high} = |dp + U_{dp} - y_{high_{MCS}}| \\ = |0.812.10^{-4}mm \leq \zeta \end{cases}$$

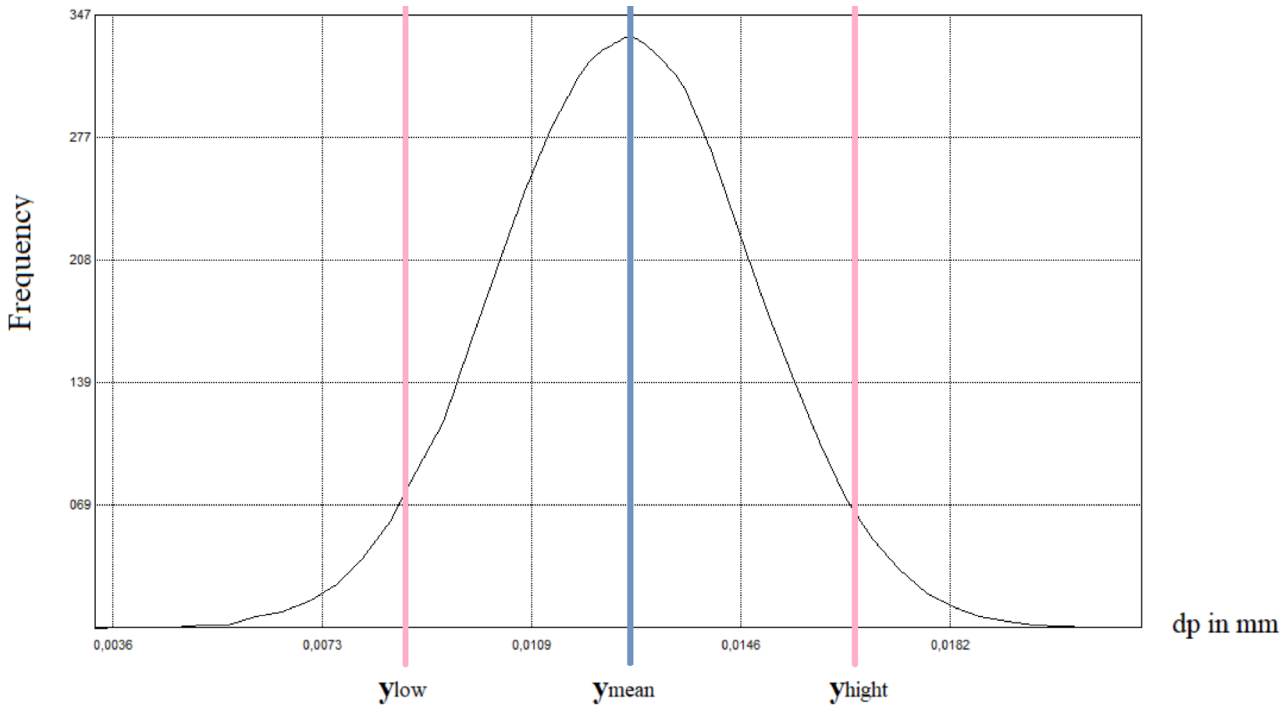

Fig. 10. Distribution Law of MCM.

The validation criterion $max\,(d_{low},\, d_{high}) \leq \zeta$ is verified, meaning that the comparison is favorable, and that the GUM framework estimating the perpendicularity uncertainty has been validated in this instance.

3.3 Conformity assessment

In order to control the perpendicularity specification (15µm tolerance limit), we calculated the consumer risk: $p_\alpha = \{dp > zi\} = 1 - \emptyset\,(z_i)$ where $z_i = \frac{Ts-dp}{U/2}$ (Tab. 5).

The risk alpha $p_\alpha = 11.3\%$ is significantly higher than the 2.3% limit specified by the standard ISO/IEC Guide 98-4. We can then conclude that the part is "not conform" to the perpendicularity specification. However, it is important to note that the conformity assessment could show different results measuring the same part and estimating the uncertainty referring to the same model, using a more performant and precise CMM, hence the necessity of an inter-laboratory comparison.

3.4 Inter-laboratory comparison

Inter-laboratory comparison (ILC) is a procedure usually used to evaluate the accuracy and the consistency of results obtained by different laboratories realizing the same measurement or test on the same sample, it can also be used in our case to validate our perpendicularity assessment model. Although there are several evaluation techniques, the calculation of the normalized error is the most often used [26,27]:

$$E_{\boldsymbol{n}} = \frac{|dp - dp_L|}{\sqrt{U(dp)^2 + U_{\boldsymbol{L}}2}} \tag{14}$$

where dp_L and $U_{\boldsymbol{L}}$ are respectively the perpendicularity error and its associated uncertainty measured by the participant laboratory. The comparison would show satisfactory results if $|E_{\boldsymbol{n}}| \leq 1$.

The ILC was realized with the Measurement Control Center (MCC) laboratory where the temperature is regulated around 20 °±2 °C, the coordinate measuring machine used is a Zeiss Duramax coupled to a Vast-xxt-tl3 type probing head on which is mounted a Tungsten Carbide stylus of effective working length EWL = 14 mm and $D = 2$ mm ruby ball diameter, altogether driven by Calypso software. The same industrial part was controlled under the same conditions and following the same measurement strategy, resulting in a perpendicularity error $dp_{\boldsymbol{MCC}} = 11.9\,\mu$m, and the mechanical part was judged to be compliant with the given specification. The CMM-associated measurement uncertainty is $U_{\boldsymbol{MCC}} = 3.3\,\mu$m estimated by manufacturer calibration. The normalized error is significantly inferior to 1:

$$E_{\boldsymbol{n}} = \frac{|0.0125 - 0.0119|}{\sqrt{0.0040^2 + 0.0033^2}} = 0.115 < 1.$$

The ILC showed very satisfactory results ($|E_{\boldsymbol{n}}| \ll 1$), we can then conclude that our CMM is accurate and that our uncertainty estimation is suitable for perpendicularity

measurement. Both laboratories evaluated the that the part is "not conform" to the given specification, however, the MCC laboratory judgment was based on the application of the acceptance criterion: $dp_L + U_L < T_s$, which in this case, did not alter the decision.

4 Conclusion

The proposed article presents a different approach for the perpendicularity conformity validation of mechanical parts using the coordinate measuring machine, by estimating the measurement uncertainty and including it in the assessment as stated in the ISO/IEC 98-4 standard. The main purpose is to provide the perpendicularity error, its associated uncertainty, and the conformity risk, directly from the set of data points.

In order to evaluate the perpendicularity error, a measuring strategy was set according to the ISO 1101 specifications, then the error mathematical model was developed (Eq. 2). To estimate it's associated uncertainty, a deconstruction of the process has been realized and the GUM propagation of uncertainties was applied, then put together in matrix form (Eq. 3). The uncertainty variance-covariance matrices were then estimated in Section 2.3, highlighting the influence of the measurement strategy parameters: the chosen fitting criterion as well as the distribution and number of the measured points. Then a Monte Carlo simulation was used to compare and validate the uncertainty estimation and showed complying results (gap less than 10^{-4}mm) which validates our developed model. The uncertainty may seem relatively big compared to the error $\frac{U(dp)}{dp} \simeq 32\%$, but it is mainly due to the low perpendicularity default compared to the capability of CMMs used.

The interlaboratory comparison was satisfactory, the normalized error confirms the concordance between the perpendicularity error and its associated uncertainty of the measured mechanical part for both laboratories. However, despite the difference of the acceptance criterion, the conformity assessment was the same.

References

1. P. Fangyu, L. Nie, Y. Bai, X. Wang, Geometric errors measurement for coordinate measuring machines, IOP Conf. Ser.: Earth Environ. Sci. **81**, 28–30 (2017)
2. J. Stone, B. Muralikrishnan, C. Sahay,Geometric effects when measuring small holes with micro contact probes, J. Res. Natl. Inst. Stand. Technol. **116**, 573–587 (2011)
3. L. Laaouina, A. Nafi, A. Mouchtachi, Application of CMM separation method for identifying absolute values of probe errors and machine errors, Int. Conf. Eng. & MIS 2016, *Agadir, Morocco*
4. S. Branko, B. Acko, S. Havrlisan, I. Matin, B. Savkovic, Investigation of the effect of temperature and other significant factors on systematic error and measurement uncertainty in CMM measurements by applying design of experiments, Measurement **158**, 107692 (2020)
5. M. Mussatayev, M. Huang, S. Beshleyev, Thermal influences as an uncertainty contributor of the coordinate measuring machine (CMM), Int. J. Adv. Manuf. Technol. **111**, 537–547 (2020)
6. M. Djezoul, E. Pairel, H. Favreliere, Influence of the probing definition on the flatness measurement, Int. J. Metrol. Qual. Eng. **9**, 15 (2018)
7. A.B. Forbes, Uncertainties associated with position, size and shape for point cloud data, J. Phys.: Conf. Ser. **1065**, 142023 (2018)
8. A.B. Forbes, Approximate models of CMM behaviour and point cloud uncertainties, Meas. Sens. **18**, 100304 (2021)
9. V.A. Rosenda, C. Costa, Souza, H.L. Costa, A. P. Piratelli-Filho, Simplified model to estimate uncertainty in CMM, J. Braz. Soc. Mech. Sci. Eng. **37**, 411–521 (2015)
10. P. Wojciech, Uncertainty of coordinate measurement of geometrical deviations, Procedia CIRP **75**, 361–366 (2018)
11. J. Wladyslaw, P. Wojcich, First coordinate measurement uncertainty evaluation software fully consistent with the GPS Philosophy, Procedia CIRP **10**, 317–322 (2013)
12. International Organization for Standardization ISO 1101: 2017–02, Geometrical product specifications (GPS) — geometrical tolerancing — tolerances of form, orientation, location and run-out
13. R. Rajamani, R. Vignesh, B. Mouliprasanth, Evaluation of uncertainty in angle measurement performed on a coordinate measuring machine, *Proceedings of the First International Conference on Combinatorial and Optimization*, ICCAP 2021, December 7–8 2021, Chennai, India
14. G. Moona, V. Kumar, M. Jewariya, H. Kumar, R. Sharma, Measurement uncertainty assessment of articulated arm coordinate measuring machine for length measurement errors using Monte Carlo simulation, Int. J. Adv. Manuf. Technol. **119**, 5903–5916 (2022)
15. JCGM 100:2008, Evaluation of measurement data — guide to the expression of uncertainty in measurement
16. JCGM 101:2008, Evaluation of measurement data — supplement 1 to the guide to the expression of uncertainty in measurement — propagation of distributions using a Monte Carlo method
17. A. Jalid, S. Hariri, A. El Gharad, J.P. Senelaer, Comparison of the GUM and Monte Carlo methods on the flatness uncertainty estimation in coordinate measuring machine, Int. J. Metrol. Qual. Eng. **7**, 302 (2016)
18. A. Jalid, S. Hariri, N.E. Laghzale, Influence of sample size on flatness estimation and uncertainty in three-dimensional measurement, Int. J. Metrol. Qual. Eng. **6**, 102 (2015)
19. ISO/IEC GUIDE 98–4:2012, Uncertainty of measurement — Part 4: role of measurement uncertainty in conformity assessment
20. ISO 17025:2017 General Requirements for Competence of Testing and Calibration Laboratories, International Organization for Standardization
21. A.B. Forbes, Sensitivity analysis for Gaussian associated features, Appl. Sci. **12**, 2808 (2022)
22. A.B. Forbes, Verification of sensitivity analysis method of measurement uncertainty evaluation, Meas. Sens. **18**, 100274 (2021)
23. K. Bahassou, A. Salih, A. Jalid, M. Oubrek, Modeling of the correction matrix for the calibration of measuring machines, Int. J. Mech. Eng. Tech. **8**, 862–870 (2017)

24. K. Bahassou Salih, M. Oubrek, A. Jalid, Measurement uncertainty on the correction matrix of the coordinate measuring machine, Int. J. Adv. Res. Eng. Tech. **10**, 669–676 (2019)
25. International Organization for Standardization ISO 10360-2:2009, CMMs Used for Measuring Linear Dimensions
26. S. Almira, H. Bašić, Proficiency testing and interlaboratory comparisons in laboratory for dimensional measurement, J. Trends Dev. Mach. Assoc. Technol. **16**, 115–118 (2012)
27. International Organization for Standardization ISO 13528:2015, Statistical Methods for Use in Proficiency Testing by Interlaboratory Comparison

Cite this article as: Nabil Habibi, Abdelilah Jalid, Abdelouahab Salih, Mohamed Zeriab Es-sadek, Perpendicularity assessment and uncertainty estimation using coordinate measuring machine, Int. J. Metrol. Qual. Eng. **14**, 12 (2023)